Dynamics and damage analysis of blueberry fruit collisions

Yudong Bao[1,2*], Jiasai Zeng[1,2], Yuying Liu[1,2]

(1. *Key Laboratory of Advanced Manufacturing and Intelligent Technology, Ministry of Education, Harbin University of Science and Technology, Harbin 150080, China*;
2. *School of Mechanical and Power Engineering, Harbin University of Science and Technology, Harbin 150080, China*)

Abstract: Fruits are easily damaged by collision during mechanical harvesting of blueberries, affecting quality. In this study, theoretical analysis, numerical simulation, and experimental verification are comprehensively employed to investigate the mechanical behavior and damage mechanism of blueberry fruit collisions. A nonlinear collision dynamics model for fruits was constructed based on Hertzian theory; the collision force is found to be related to the mass, the coefficient of restitution, the material properties of the collided object, and the collision velocity. A discrete element simulation model was created, as was a finite element simulation model. The fruit collision type was determined, and the analysis showed that when the collision velocity of the fruit-rigid plate collision model was increased from 1 m/s to 3 m/s, the peak contact stress increased from 64 000 Pa to 110 000 Pa, the peak collision force increased from 1.85 N to 6.75 N, and the damage volume increased from 152.72 mm^3 to 459.42 mm^3, which is more likely to trigger compared to the fruit-fruit collision model plastic deformation. Through the collision test it was determined that blueberry fruit can withstand a maximum collision force in the range of 2.00-3.00 N. More than 300 mm of drop height will cause the damage surface ratio to increase dramatically. The results of this study identified the key factors and thresholds affecting damage, providing a theoretical basis for reducing the damage rate of blueberry fruit and also providing a reference for the mechanical harvesting of other berry fruits.

Keywords: blueberry, mechanical harvesting, collision mechanics, fruit damage
DOI: 10.25165/j.ijabe.20261902.10030

Citation: Bao Y D, Zeng J S, Liu Y Y. Dynamics and damage analysis of blueberry fruit collisions. Int J Agric & Biol Eng, 2026; 19(2): 39–48.

1 Introduction

In recent years, the domestic blueberry industry has been gradually expanding, but blueberries and other berries are delicate, and in the process of mechanical harvesting, it is easy to cause damage due to collision. Damage not only affects the appearance and quality of the fruit, but may also trigger decay and reduce the market value of the fruit[1-3]. Therefore, it is important to study the collision mechanical behavior and damage mechanisms of blueberry fruit during mechanical harvesting to reduce fruit damage and improve fruit quality[4].

Currently, in collision mechanics, Hu and Guo[5] proposed a new dissipative contact force model based on Hertz’s contact law, which can be used to calculate the energy loss due to damping forces using an approximate function that represents the relationship between deformation velocity and deformation. Alaci et al.[6] investigated the analytical solution for the central collision of two viscoelastic spheres, emphasizing the influence of the coefficient of recovery on all collision characteristics, and proposed a simplified algorithm for the calculation of viscoelastic impact parameters, which can be generalized to nonlinear viscoelastic-plastic impact processes. Zheng et al.[7] also used the finite element method to analyze the relationship between normal and tangential forces and displacement between a viscoelastic sphere and a rigid plane, and proposed a new set of semi-analytical models for normal and tangential forces, which can be used to understand the nature of the mechanics and mechanism of the collision process. Lapshin et al.[8] developed a mechanobiological three-mass viscoelastic-plastic model that describes the transition conditions from elastic to plastic deformation and from loading to unloading phases under impact interactions with surfaces, which can be used in practical applications to improve the accuracy and reliability of the simulation of impact processes.

In fruit damage analysis, Yousefi et al.[9] determined the bruised area of pear fruit by drop test and predicted it by the finite element method. The results of the study can be used to predict the damage characteristics of pear fruit drop and the critical drop height of the test. Dintwa et al.[10] analyzed the dynamics of apple fruits colliding with each other or with a rigid surface using a finite element model, and concluded from dynamic collision tests that the magnitude of the energy loss depends on the elastic properties of the material, the geometry of the colliding object, and the collision velocity. Wang et al.[11] studied the impact behavior between fruits and rigid plates using two varieties of lychee as test materials, and successfully fitted the relationship between impact energy and depth of compression as well as compressed volume and degree of damage for both varieties, which can be used to predict the degree of damage. Zhang et al.[12] developed an elastic impact model and a model considering energy dissipation to describe the deformation behavior of lychee during collision damage so that the impact force, deformation, and contact time could be predicted. Du et al.[13] modeled kiwifruit as a multi-scale pulp and skin, and predicted kiwifruit damage susceptibility using finite element methods, obtaining that the horizontal direction is more likely to cause damage than the vertical heel. Hou et al.[14] dissected blueberry structures, developed empirical models to predict bruise

Received date: 2025-07-16 **Accepted date:** 2025-12-11
Biographies: Jiasai Zeng, MS, research interest: agricultural machinery, Email: 2021277885@qq.com; **Yuying Liu**, MS, research interest: agricultural machinery, Email: 18245419728@163.com.
***Corresponding author: Yudong Bao**, Professor, research interest: agricultural equipment and intelligent technology. School of Mechanical Engineering, Harbin University of Science and Technology, Harbin 150080, China. Tel: +86-451-86390588, Email: baoyudong@hrbust.edu.cn.

susceptibility for each contact material, and used a data-driven computational approach to propose predictive tools that can accurately quantify fruit bruising.

Through the above research, it is found that the study of fruit collision needs to be based on a reasonable mechanical model, and at present, the research on the impact damage of apples, pears, and other fruits with strong impact resistance is more in-depth, while the research on blueberries and other berry fruits is relatively less. Most of the studies have used numerical simulation methods such as finite element simulation and crash tests to fruitfully predict the mechanical changes and damage during the collision.

The research of this paper was carried out through a combination of theoretical analysis, numerical simulation, and experimental verification. Based on the Hertzian theory, a dynamic model of nonlinear collision of blueberry fruit was established to derive the influencing factors affecting the magnitude of the collision force. Through discrete element simulation, finite element simulation, and fruit collision test, the collision of fruit in mechanical picking and the influence of different factors on the collision process of fruit were investigated to analyze the dynamic response characteristics of the fruit under the impact load, and to reveal the mechanism of fruit collision mechanical behavior and damage. This study can provide a theoretical basis for the design of blueberry harvesting equipment, reduce the rate of fruit damage and improve the economic value of the fruit, and can also provide a reference for the design of harvesting equipment for other berry fruits[15,16].

2 Constructing a nonlinear collision dynamics model for blueberry fruits

The principle of blueberry vibratory mechanical harvesting is to transfer the vibration energy generated by the shaker to the fruit tree. When the vibration energy exceeds the connecting force between the fruit stalk and the fruit, it will cause the fruit to fall off, and ultimately fall to the fruit catching plate[17], as shown in Figure 1 below. The compressive or impact loads applied to the fruit during abscission are considered to be the type of behavior that is viscoelastic[18], so the viscoelastic behavior of blueberry fruit during collision is usually non-linear during the actual harvesting process[19]. Therefore, in this paper, a nonlinear dynamics model will be developed to reveal the complex mechanical mechanism of the collision of fruit mechanical harvesting.

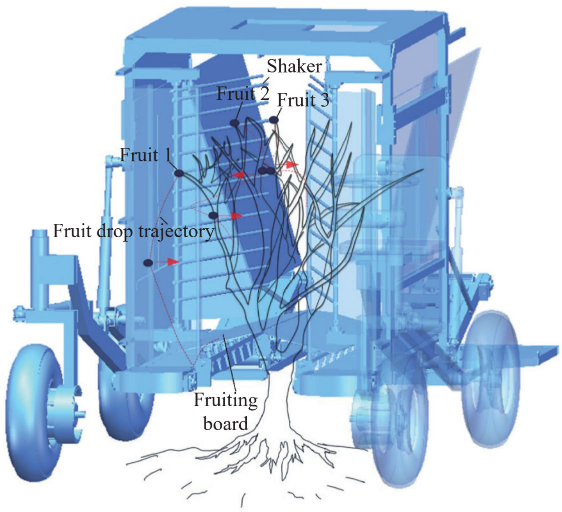

Figure 1 The operational principle of the vibrating blueberry harvester

During the collision process, a Hertz damping model based on Hertz's contact law is used to describe the collision forces and deformations of the fruit throughout the collision process at a given moment t:

$$F(t) = K\delta(t)^{3/2} + \zeta\delta(t)^{3/2}v(t) \tag{1}$$

where, $F(t)$ is the collision force at moment t, N; $\delta(t)$ is the deformation at moment t, m; $v(t)$ is the velocity at moment t, m/s; K is the Hertzian contact stiffness; and ζ is the damping constant.

To ensure that Equation (1) is dimensionally consistent, the damping term $\zeta\delta^{3/2}(t)v(t)$ must have the units of force (N); it follows that $[\zeta]\cdot \mathrm{m}^{1.5}\cdot(\mathrm{m/s}) = \mathrm{N}$, hence the damping constant has units $[\zeta] = \mathrm{N\cdot s\cdot m^{-2.5}}$. Similarly, since the elastic term $K\delta^{3/2}(t)$ also represents a force, the Hertzian stiffness K has units $[K] = \mathrm{N\cdot m^{-1.5}}$.

This expression describes the nonlinear viscoelastic collision process. The parameter K depends on the material properties and radius of the collided object and can be expressed as,

$$K = \frac{4}{3\pi(h_1+h_2)}\sqrt{\frac{R_1R_2}{R_1+R_2}} = \frac{4}{3\pi(h_1+h_2)}\sqrt{R_1} \tag{2}$$

where, R_1 is the radius of the impacting fruit, m; R_2 is the radius of the collided plate, m; the radius of the fixed plate is considered to be ∞.

The material parameters h_1 and h_2 are as follows:

$$h_i = \frac{1-\mu_i^2}{\pi E_i};\ i = 1,2 \tag{3}$$

where, E_1 is the modulus of elasticity of the colliding fruit, Pa; E_2 is the modulus of elasticity of the collided object, Pa; μ_1 is the Poisson's ratio of the colliding fruit; μ_2 is the Poisson's ratio of the collided object.

Considering the effect of damping on fruit impact, at a given moment, the initial kinetic energy before impact is equal to the sum of the potential energy accumulated during compression, and the work done by damping and the residual kinetic energy can be expressed as,

$$E_k = \int_0^{\delta(t)} K\delta(t)^{3/2}\mathrm{d}\delta + \Delta E(t) + \Delta E_k(t) \tag{4}$$

where, $\Delta E(t)$ is the dissipated energy at moment t, J; $\Delta E_k(t)$ is the residual kinetic energy at moment t, J.

Most of the modulus of elasticity values after the collision were smaller than before the collision, suggesting that the impact disrupted or altered the cellular structure of the fresh fruit, and that these changes may have resulted in partial dissipation of energy, which, in the case of the fruit, ultimately leads to fruit damage. Therefore, the total dissipated energy ΔE during the collision is as follows:

$$\Delta E = \Delta E_1 + \Delta E_2 \tag{5}$$

where, ΔE_1 is the dissipated energy due to damping, J; ΔE_2 is the dissipated energy due to reduction of elastic modulus, J.

The dissipated energy due to damping and the velocity of the fruit at a given moment can be expressed as,

$$\Delta E_1 = \oint \zeta\delta(t)^{3/2}v(t)\mathrm{d}\delta = \frac{4}{15}(1+e)\zeta v_0\delta_{\mathrm{m}}^{5/2} \tag{6}$$

$$v(t) = \begin{cases} v_0\left[1-\left(\dfrac{\delta(t)}{\delta_m}\right)^{5/2}\right]^{1/2};\ v(t) > 0 \\ v_p\left[1-\left(\dfrac{\delta(t)}{\delta_m}\right)^{5/2}\right]^{1/2};\ v(t) < 0 \end{cases} \tag{7}$$

where, v_0 is the initial relative velocity, v_p is the separation relative velocity, and e is the coefficient of restitution.

The energy dissipated during the collision is absorbed by the fruit and can be expressed as,

$$\Delta E = \frac{m_1 m_2}{2(m_1+m_2)}(1-e^2)v_0^2 = \frac{m_1}{2}(1-e^2)v_0^2 \tag{8}$$

where, ΔE is the energy absorbed by the fruit, J; m_1 is the mass of the colliding fruit, kg; m_2 is the mass of the plate subjected to the collision, kg; and the weight of the fixed plate is considered to be ∞.

The dissipated energy due to the reduction of the modulus of elasticity is considered to be the difference between the potential energy of the approach phase (ΔE_{21}) and the potential energy of the rebound phase (ΔE_{22}), determined by the contact stiffness of the fruit before and after the impact, respectively. Then, the energy ΔE_2 can be described as,

$$\Delta E_2 = \Delta E_{21} - \Delta E_{22} = \frac{2(K_1-K_2)\delta_{\mathrm{m}}^{5/2}}{5} \tag{9}$$

where, K_1 is the Hertzian contact stiffness before collision, N/mm; K_2 is the Hertzian contact stiffness after collision, N/mm.

Combining Equation (4) and Equation (6), the maximum deformation can be written as,

$$\delta_{\mathrm{m}} = \left(\frac{15E_k}{4\zeta v_0 + 6K_1}\right)^{2/5} \tag{10}$$

Combining Equation (6), Equation (8), and Equation (10), the damping constant is obtained:

$$\zeta = \frac{3(K_2 - e^2K_1)}{2e(1+e)v_0} \tag{11}$$

The validity of the damping constant derived in Equation (11) is verified through its dimensional consistency and physical rationality. In terms of dimensional analysis, Equation (11) gives $[\zeta] = \frac{\mathrm{N\cdot m^{-1.5}}}{\mathrm{m/s}} = \mathrm{N\cdot s\cdot m^{-2.5}}$, which is consistent with the dimension of $[\zeta]$ obtained above, indicating that the dimensions are identical. Furthermore, assuming that the stiffness remains unchanged before and after impact, i.e. $K_1 = K_2 = K$, Equation (11) can be simplified to the generalized form of the classical L-N model, $\zeta_1 = \frac{3K(1-e)}{2v_0}$. This formulation correctly captures the expected physical limits: as $e\to 1$ (perfectly elastic), $\zeta \to 0$, and as $e \to 0$ (perfectly plastic), $\zeta\to\infty$, which is consistent with nonlinear viscoelastic impact theory. Equation (11) contains different stiffness parameters K_1 and K_2, so energy is dissipated not only by viscous damping but also by stiffness degradation. This captures the extra energy loss from irreversible damage to the fruit tissue and makes the model suitable for the elastoplastic behavior of fruits.

Finally, the collision force for a given moment is determined based on the Hertzian damping model:

$$F(t) = \begin{cases} K_1\delta(t)^{3/2} + \dfrac{3(K_2-e^2K_1)\delta(t)^{3/2}}{2(1+e)}\left[1-\left(\dfrac{\delta(t)}{\delta_m}\right)^{5/2}\right]^{1/2}; & v(t)>0 \\ K_1\delta(t)^{3/2} - \dfrac{3eK_2(1-e)\delta(t)^{3/2}}{2}\left[1-\left(\dfrac{\delta(t)}{\delta_m}\right)^{5/2}\right]^{1/2}; & v(t)<0 \end{cases} \tag{12}$$

The collision force is related to the deformation, the coefficient of recovery, and the velocity, so that the maximum collision force does not occur at a certain moment, but is determined based on all parameters. Based on Equation (1), with the basic kinetic equation of the contact collision model $m\ddot{\delta} + k\delta^n + \lambda\delta^n\dot{\delta} = 0$, the kinetic equation of the fruit collision is obtained by considering the dissipated energy caused by the change of damping and the reduction of elastic modulus before and after the fruit collision:

$$\begin{cases} m\ddot{\delta}(t) + \zeta\delta(t)^{3/2}\dot{\delta}(t) + K_1\delta(t)^{3/2} = 0 \\ \delta(0) = 0 \\ \dot{\delta}(0) = v_0 \end{cases} \tag{13}$$

The complex contact deformation and dynamic behavior of fruits in the collision process were analyzed by collision contact force analysis and nonlinear collision dynamics model of fruits, and it was obtained that the collision force was related to the mass, the coefficient of recovery, the material properties of the object subjected to the collision, and the collision velocity. The mass and coefficient of recovery are determined by the internal properties of the blueberry, while the material properties of the collided object and the collision velocity are determined by external factors.

3 Simulation analysis of blueberry fruit collision

3.1 Creation of a discrete meta-simulation model of blueberry

To study blueberry motion after vibration shedding, EDEM was used for discrete element simulations. Each blueberry was modeled as a single sphere with an average radius of 8.5 mm, and the size distribution followed a normal probability density function based on measured fruit sizes. This is a geometric simplification that does not fully represent the irregular surface of real blueberries. Therefore, the DEM model is used only to analyze the overall motion trajectories of detached blueberries and identify the dominant contact types during detachment. Material and contact parameters of the harvester and blueberries were taken from Bao et al.[20], as listed in Table 1.

Table 1 Setting of various material parameters

Parameters	Blueberries	Harvesters
Poisson's ratio	0.30	0.28
Shear modulus/Pa	2.9×10^8	7.9×10^{10}
ρ/kg·m^{-3}	1160	7820
Coefficient of static friction between harvester and blueberry	0.3	0.4
Coefficient of dynamic friction between harvester and blueberry	0.04	0.07
e	0.2	0.5

Since the interaction between blueberries and the components of the harvester and the blueberry fruit occurs during the harvesting process, but there is no adhesion force, the Hertz-Mindlin (no slip) contact model can be used to describe the blueberry harvesting process, and the harvesting process simulation parameter is set to have a total time length of 1.5 s, and the interval between data outputs is 0.005 s. For meshing, two times the minimum particle radius was selected as the standard size of the grid cells.

This study takes the eight-year-old Duke blueberry tree as an example. The average height of the fruit tree is 1200 mm. Based on its geometry, four circular virtual planes with a radius of 500 mm were created to define the region of the particles generated. Considering the fruit concentration zone of the blueberry tree, the heights of the virtual planes above the ground were set to 440 mm, 620 mm, 800 mm, and 980 mm. In this study, the dynamic particle generation was selected, the number of particles generated in each plane was 200, and the particle shedding speed was set to 1 m/s for simulation analysis to obtain the trajectory and distribution.

3.2 Analysis of discrete element simulation results for fruit harvesting

Using EDEM's post-processing Selections module to randomly select four particles to show the motion trajectory of the harvesting process in a streamlined state, the simulation results obtained are shown in Figure 2. Observation of the movement trajectory at a drop height of 440 mm reveals that all the fruits fall directly to the bottom. At a drop height of 620 mm, the fruit falls off and collides with the side wall to the bottom of the harvester. At a falling height of 800 mm, the fruit falls to the bottom after falling off and colliding with the finger rows of the harvester, and the fruit falls to the bottom of the harvester after falling off and colliding with the fruit. At a falling height of 980 mm, the trajectory of the fruit does not have a certain regularity, and all types of collisions may occur.

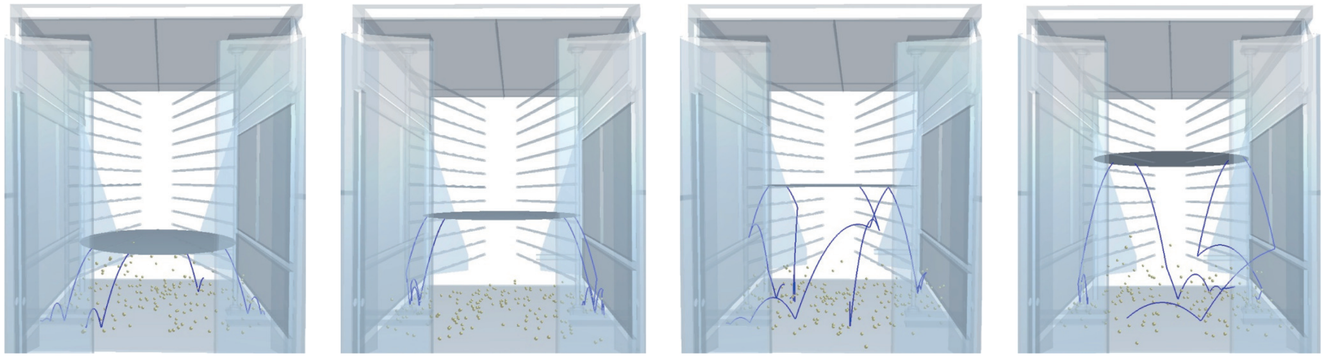

a. Particle trajectory at height 440 mm b. Particle trajectory at height 620 mm c. Particle trajectory at 800 mm height d. Particle trajectory at height 980 mm

Figure 2 Trajectories of particles at different heights

3.3 Creation of a finite element model of the blueberry

The pulp of blueberries is considered to be a homogeneous, isotropic elastoplastic material, and the pericarp is considered to be a linear elastic material. Therefore, the isotropic hardening model is chosen as the intrinsic model of the elastoplastic material in the finite element simulation, following the isotropic hardening law.

Material properties of blueberries can be obtained from experimental data or literature. The tissue of blueberry is composed of peel, pulp, and seed, and the material properties of each part should be defined separately; the material properties of peel and pulp are listed in Table 1.

A multi-scale geometrical model is constructed based on the structure of blueberries in the shape of an ellipsoid, whose dimensions are defined by experimental measurements, as listed in Table 2.

Table 2 Definition of blueberry fruit size

Contents	Length/mm	Width/mm	Height/mm	Thickness/mm
Pericarp	16.50±1.64	16.50±1.64	14.60±0.95	0.15±0.01
Pulps	16.20±1.63	16.20±1.63	14.30±0.94	-

Based on the above data, the geometric model of blueberry was created in Space Claim software, the volume of the blueberry model is about 2083.42 mm^3, and its profile is shown in Figure 3. The display dynamics analysis module was created in Ansys software to define the peel and pulp material properties of the fruit and import the geometric model.

According to the results of the discrete element simulation analysis, the fruit-rigid plate and fruit-fruit collision finite element models were created, respectively, after importing the geometric model. For the fruit-rigid plate collision model, the rigid plate is set in the shape of a rectangle, and the rigid plate is stationary concerning the fruit throughout the collision process, so fixed supports are added to it. For the fruit-fruit collision model, the two fruits are moving in opposite directions during the collision process, so no boundary conditions are set. In this study, the blueberry peel and flesh were discretized with tetrahedral finite elements and the rigid plate with hexahedral elements. A global adaptive element size of 0.50 mm was applied to both the blueberry and the rigid plate, while the thin peel layer was locally refined via adaptive sizing to a characteristic element size of approximately 0.06 mm.

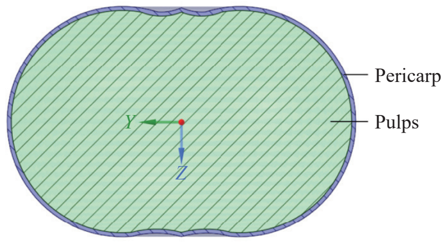

Figure 3 The cross-sectional view of the blueberry geometric model

Due to the randomness of the speed at which blueberries are subjected to vibration and fall, three collision velocity levels of 1 m/s, 2 m/s, and 3 m/s were set in this study. The length of each simulation was set to 0.01 s, the output of the simulation and analysis process is 100 isometric points, and the data are collected and analyzed at the end of the simulation.

3.4 Finite element simulation analysis of blueberry fruit collision

3.4.1 Analysis of the fruit collision process

The simulation results show that at a collision velocity of 1 m/s, neither the fruit-rigid plate collision model nor the fruit-fruit collision model undergoes plastic deformation. At a collision speed of 3 m/s, both models deform plastically, and only at a collision speed of 2 m/s is there a significant difference between the two collision models, with plastic deformation occurring in the fruit-rigid plate collision model, but not in the fruit-fruit collision model. Therefore, this paper selects the collision speed of 2 m/s to simulate the collision process for detailed analysis. By comparing the simulation results of the two collision models, the difference can be obtained by the collision object material properties of the impact on the collision of the blueberry fruit.

Figure 4 shows the simulation results of the fruit-rigid plate collision model. The fruit equivalent stress cloud map shows that the maximum stress of the fruit reaches about 99 515 Pa during the collision, and it is concentrated in the contact area and spreads to the interior; the fruit plastic strain cloud map reveals the local permanent deformation caused by the collision, with a peak value of about 0.031; the peel equivalent stress cloud map reveals that the maximum stress of the fruit peel reaches about 58 873 Pa, and is mainly distributed on both sides of the contact area; the flesh equivalent stress maps show that the maximum stress in the flesh reaches 99 515 Pa, and with the deepening of the collision, the pressure is transferred to the inner part of the fruit. When the collision speed is 2 m/s, the maximum stress on the fruit exceeds the yield stress of the pulp of (90 000±1900) MPa, plastic deformation occurs, and the damage mainly occurs in the pulp.

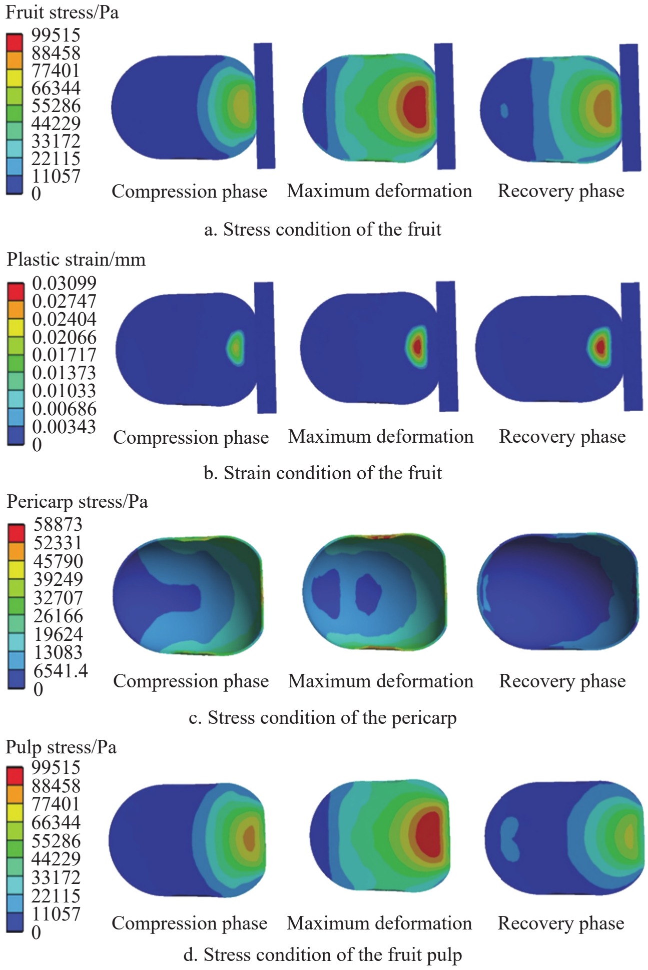

a. Stress condition of the fruit

b. Strain condition of the fruit

c. Stress condition of the pericarp

d. Stress condition of the fruit pulp

Figure 4 Fruit-to-rigid-plate simulation collision process

Figure 5 shows the simulation results of the fruit-fruit horizontal collision model. Fruit equivalent stress maps showed that the maximum stress reached about 72 668 Pa; the pericarp equivalent stress maps show that the maximum stress is about 29 510 Pa; the fruit pulp equivalent stress cloud map shows that the maximum stress is about 72 668 Pa. The analysis revealed that the maximum stress on the fruit did not exceed the yield stress of the pulp and that the collision did not result in plastic strain.

At a collision velocity of 2 m/s, the difference between the simulation results of the two collision models is due to the difference in the material properties of the collided objects. In the fruit-fruit collision model, the hardness and modulus of elasticity of the two fruits are similar, and the collision energy can be more uniformly dispersed between the two fruits, which reduces the local stress concentration phenomenon. In the fruit-rigid plate collision model, the high stiffness of the rigid plate causes the collision energy to be concentrated in the fruit-contact region, resulting in greater stresses on the flesh and greater susceptibility to plastic deformation. Therefore, the collision analysis of the fruit-rigid plate collision model at different speeds will be the focus of the following study.

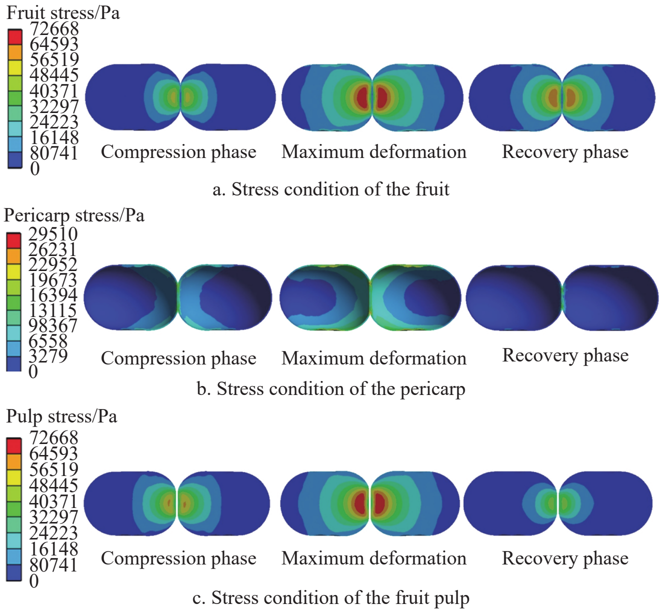

a. Stress condition of the fruit

b. Stress condition of the pericarp

c. Stress condition of the fruit pulp

Figure 5 Fruit-to-fruit simulation collision process

3.4.2 Mechanical analysis of fruit-rigid plate collisions

The stresses and collision forces in the fruit for different collision speeds in the fruit-rigid plate collision model are shown in Figure 6. From the stress curves, it can be seen that the peak value of the contact stress increases significantly as the collision velocity increases from 1 m/s to 3 m/s. The peak stress was about 64 000 Pa at 1 m/s, rising to about 92 000 Pa at 2 m/s and approaching 110 000 Pa at 3 m/s. This suggests that the higher the collision velocity, the higher the relative impact between the fruit surface and the collision surface, which can lead to higher stress concentrations. When the initial velocity increases from 1 m/s to 2 m/s, it can be seen that the fruit starts to deform plastically when combined with the yield stress of the fruit.

From the collision force curve, the peak contact force increases markedly with impact velocity, with peak values of about 1.85, 4.26, and 6.75 N at 1, 2, and 3 m/s, respectively, and the peak occurs earlier as the impact velocity increases. This behavior is consistent with the nonlinear viscoelastic collision model in Section 2. According to Equation (1), the contact force is the sum of an elastic term governed by the instantaneous deformation and a damping term governed by the deformation rate. A higher initial impact velocity v_0 gives a larger initial kinetic energy $\frac{1}{2}mv_0^2$, leading to greater deformation and deformation rates during contact. Consequently, both the elastic and damping contributions increase, so the collision force rises more rapidly and reaches its maximum earlier. At the same time, the larger damping term at higher velocities results in stronger energy dissipation and a shorter decay time of the collision force toward a steady state, indicating that internal deformation and energy dissipation become more rapid and concentrated under high-speed impact.

3.4.3 Fruit-rigid plate collision damage analysis

Considering the relationship between material damage and irreversible permanent deformation, this study used equivalent plastic strain (PEEQ) as a representative indicator of fruit damage. PEEQ is used to quantify the cumulative plastic deformation or strain experienced by a material during a specific loading or deformation process. Since damage to the fruit only occurs when a certain level of the impact energy is exceeded, the damage region is determined by identifying the region where the PEEQ value exceeds a specified threshold. Figure 7 shows the damage volume of the fruit extracted from the simulation results in the fruit-rigid-plate collision model at an initial velocity of 2 m/s. According to the multiscale computational study on bruise susceptibility of blueberries under mechanical impact by Hou et al.[14], the onset of internal bruising corresponds to equivalent plastic strains on the order of 10^{-2}; therefore, the PEEQ threshold was set to 0.01 in this work.

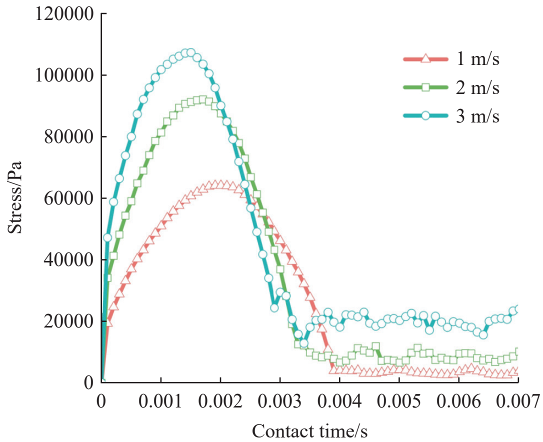

a. Stress curve

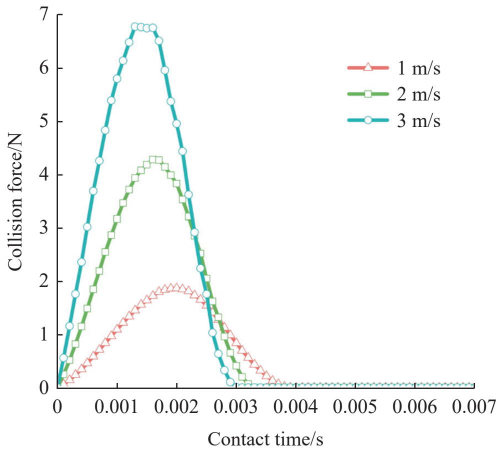

b. Collision force curve

Figure 6 The stress and collision forces of fruits at different speeds

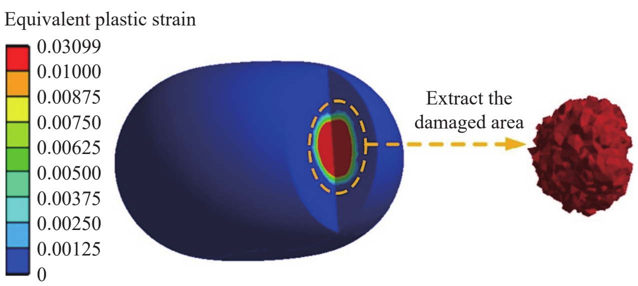

Figure 7 Fruit damage volume plot

Figure 8 demonstrates the effect of collision velocity on the damage characteristics of blueberry fruits through the evolution of the internal damage volume of the fruits with time at different velocities (1 m/s, 2 m/s, 3 m/s).

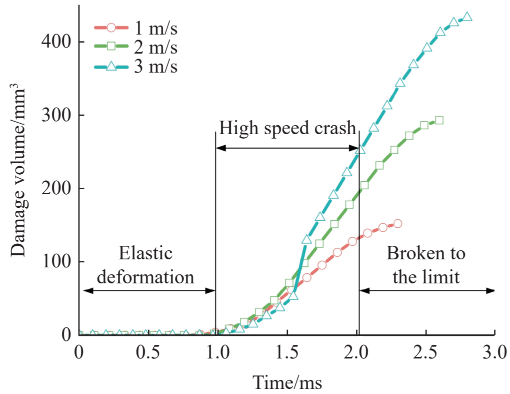

Figure 8 The evolution process of collision damage volume

In the initial stage (0-1 ms) of the damage accumulation process, the damage volume grows slowly and all three curves are at a low level; elastic deformation mainly occurs in blueberry fruits at this stage. During the rapid growth phase (1-2 ms), damage accumulation accelerates and the three curves begin to separate, showing a significant effect of speed on the rate of damage volume accumulation, with high-speed collisions resulting in much higher damage volumes than low speeds. In the saturation stage (2-3 ms), the damage volume gradually tends to stabilize, but the high-speed collision curve still maintains a significant growth, the damage accumulation rate slows down with the reduction of speed, and the internal breakage of the fruit due to high-speed collision almost reaches its limit. The maximum damage volume of blueberry fruits at speeds of 1 m/s, 2 m/s, and 3 m/s were 152.72 mm^3, 293.21 mm^3, and 459.42 mm^3, respectively. The model volume was known to be 2083.42 mm^3, and thus the extent of damage was 7.33%, 14.07%, and 22.05%, respectively.

The results show that the collision speed in the fruit-rigid plate collision model is a key factor affecting the degree of fruit damage, and the high-speed collision leads to a significant expansion of the damaged area inside the fruit. The damage volume increased non-linearly with time, with slow growth at the beginning of the collision and accelerated accumulation of damage at the later stage, which may be related to the biomechanics of the fruit.

4 Blueberry fruit-rigid plate crash test

4.1 Test materials and methods

The test rig required for the crash experiments is shown in Figure 9 and consists of a suspension, a high-speed camera model (IDT's Y4-S3 model), a force transducer, and a data acquisition model.

The pendulum wire suspended on the suspension makes the blueberry fruits fall at different heights, the high-speed camera model records the movement state of the fruits during the whole collision process in real time, and the force data acquisition model records the impact force during the collision process in real time. The SSF7427 force load cell is selected to measure the collision force, and in order to meet the requirements and obtain as many sampling points as possible, the NI-USB-6210 data acquisition card is selected for the signal acquisition of the contact force.

For the test, blueberry fruits were suspended from the suspension with a fishing line, and the fruits were dropped from falling heights of 100 mm, 200 mm, 300 mm, 400 mm, and 500 mm to obtain different collision speeds. The collision process was recorded at 2000 fps, capturing images of 1024×1024 pixels, and the hand was released to make the fruit swing and fall until collision with the force sensor, which recorded the contact force-time data of the fruit collision in real time during the collision process, and then transmitted to the computer via the amplifier and the data acquisition card for storage. Fifteen fruits were tested at each height, and the deformation and speed of the fruits before and after the collision were measured using the captured images.

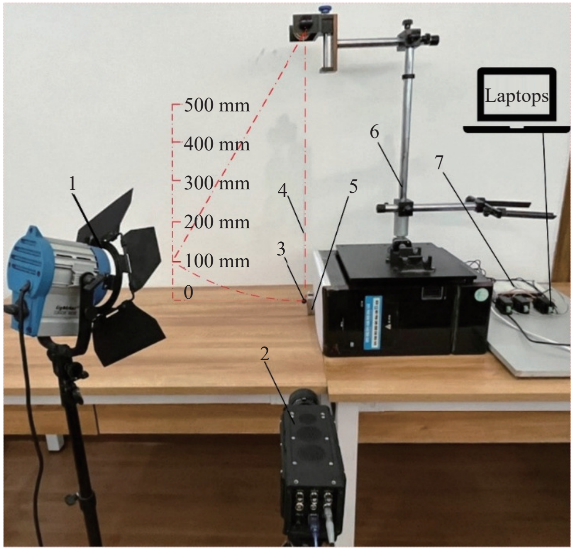

1. Fill light 2. High-speed camera 3. Blueberry fruit 4. Fishing line 5. Force sensor 6. Suspension 7. Data acquisition card

Figure 9 Crash test rig

4.2 Test crash velocity analysis

As shown in Figure 10, after the initial contact between the fruit and the sensor plane, the fruit deformation increases with time and reaches a maximum value at the end of the compression phase. Since the sensor material is stainless steel and the stiffness is much larger than the fruit stiffness, the deformation of the sensor plane is not taken into account, so the maximum deformation δ_m for the blueberry fruit collision can be expressed as:

$$\delta_m = |y_2 - y_3| \tag{14}$$

where, y_2 is the transverse diameter of the fruit before collision, mm, and y_3 is the transverse diameter of the fruit at the end of the compression phase, mm.

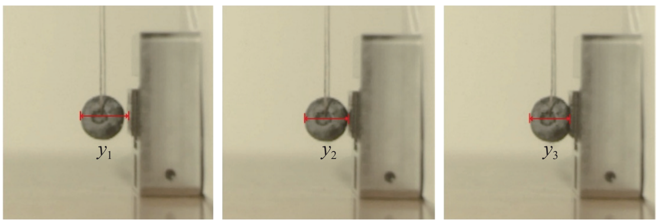

a. Pre-introduction contact b. Post-initial exposure c. The end of the compression phase

Figure 10 Fruit test collision process

The initial collision velocity v_0 is usually calculated based on the kinetic energy converted from the potential energy generated by the falling height of the fruit, but the change in the size of the fruit and the location where the collision occurs may cause errors. In this study, fruit motion was recorded with a high-speed camera operating at 2000 fps (time resolution 0.5 ms). For each test, 4-6 consecutive frames immediately before the first visible contact between the fruit and the force sensor (a time window of about 2.0-3.0 ms) were selected, and Equation (15) was used to compute the average velocity v over this short free-swing interval. Because the motion in this stage is governed primarily by gravity, the change in velocity within 2.0-3.0 ms is negligible compared with the overall impact velocity; therefore, this average velocity v was taken as the initial pre-impact relative velocity v_0.

$$v = \frac{(y_1 - y_2)f}{n} \tag{15}$$

where, y_1–y_2 is the displacement of the fruit between the two frames before the collision, mm, n is the frame difference between the two frames, and f is the frame rate of the high-speed camera.

Theoretically, the smaller the value of n, the higher the accuracy. Post-collision relative velocity is usually calculated by measuring the rebound angle with a high-speed camera. The vibration of the line used to hang the fruits may lead to measurement errors, so the separation relative velocity is also determined by the method described above.

Crash tests were conducted on blueberry fruit at five heights, and the test data are shown in Table 3.

Table 3 Collision test results (mean±standard deviation)

Drop height/ mm	Mass/g	Radius/mm	Initial relative velocity V_0/m·s^{-1}	Separation relative velocity V_p/m·s^{-1}
100	2.63±0.17	7.75±0.33	1.29±0.06	0.65±0.06
200	2.60±0.21	7.92±0.32	1.80±0.06	0.84±0.08
300	3.05±0.15	8.07±0.61	2.21±0.10	0.93±0.10
400	2.91±0.15	7.82±0.40	2.66±0.06	0.99±0.08
500	3.22±0.12	8.15±0.51	3.32±0.16	1.13±0.07

After the initial relative velocity and separation relative velocity are known, the coefficient of restitution at different heights is obtained by the formula for the coefficient of recovery, $e = \frac{v_p}{v_0}$. As shown in Figure 11, the coefficient of restitution decreases monotonically as the drop height increases from 100 to 500 mm. From a mechanics perspective, e represents the ratio of the kinetic energy recovered after impact to the initial kinetic energy before impact.

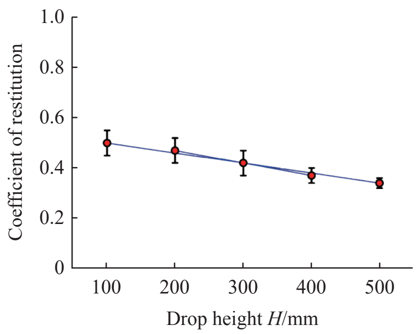

Figure 11 Relationship between drop height and coefficient of recovery

At low drop heights, the impact velocity and contact stress are relatively small and remain below the yield stress of the fruit flesh. The fruit therefore undergoes predominantly elastic deformation, with almost no visible surface indentation or bruising. As the drop height increases, the impact velocity and contact stress rise sharply, and the fruit enters an elastic-plastic deformation regime. Part of the deformation then becomes irreversible, which macroscopically manifests as local tissue collapse and softening, dark internal bruising, and, in severe cases, juice redistribution and exudation along internal cracks. As a result, a larger fraction of the impact energy is dissipated through irreversible deformation and internal damage rather than being converted back into rebound kinetic energy, leading to a progressive decrease in e with increasing drop height.

It is precisely this impact-induced variation of the coefficient of restitution that gives rise to the nonlinear elastoplastic response of blueberries under impact loading.

4.3 Test crash force analysis

The collision force data for blueberries at different drop heights are shown in Figure 12. As the drop height increases, the collision force exhibits a clear increasing trend. At heights of 100 mm and 200 mm, the peak forces are relatively small, the distributions are narrow, and the force fluctuations are gentle, indicating that at low heights the blueberry structure can effectively absorb the impact and gradually recover. At heights from 300 mm to 500 mm, the peak forces increase markedly, the curves become wider, and the fluctuations become more pronounced. This behavior reflects that, at higher drop heights, the fruit undergoes more pronounced internal compression, deformation, and even structural damage.

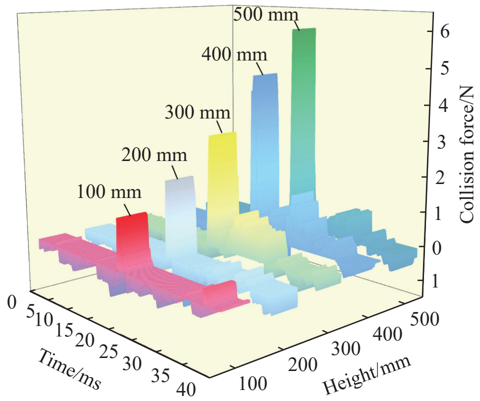

Figure 12 Collision force at different heights

Moreover, as the drop height increases, the peak force in the experiments tends to occur slightly later, which is opposite to the finite element prediction under idealized conditions. This apparent discrepancy is mainly attributed to practical experimental factors. First, the fruits are suspended by a fishing line and inevitably swing before impact, so the collisions are rarely perfectly central or normal and part of the kinetic energy is converted into rotational motion. Second, the compliance of the sensor assembly, together with the bandwidth and filtering of the measurement system, can broaden the measured force pulse and slightly delay the recorded peak. Third, differences in size, firmness, and maturity among individual fruits also influence the detailed shape and timing of the measured force-time curves.

It can be deduced from the test data that the maximum impact force that blueberry fruit can withstand is approximately 2.00-3.00 N. If this value is exceeded, the impact force exceeds the structural tolerance of the blueberry fruit and significant irreversible deformation or damage may begin to occur within the blueberry. This force value can be used as an important reference indicator for assessing the tolerance of blueberries during mechanical picking.

4.4 Crash test fruit damage analysis

The post-test blueberry fruit was placed on a test bench and left at room temperature for 24 h to ensure that the damage was fully formed, after which they were cut along the middle of the fruit and photographed and recorded, with the damaged areas (i.e., discolored areas) in each image manually extracted and marked in red. The area of the damaged area was measured to determine the fruit damage surface ratio S_r, and the results are shown in Figure 13. Since the overall damage volume of blueberries is difficult to measure, this paper approximates the experimentally measured damage surface ratio to the degree of blueberry damage. After analyzing the results, it can be concluded that the higher the drop height, the larger the damaged area. At heights above 300 mm, the damage surface ratios reached 20.05%, 25.84%, and 31.52%, respectively, and the increasing trend of damage surface ratios from 200 mm to 300 mm was significant, indicating that it was difficult to maintain the integrity of the fruits at heights higher than 300 mm, and the risk of breakage increased substantially.

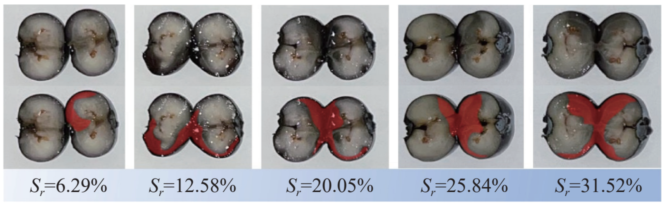

Figure 13 Fruit damage surface ratio

In the box plots in Figure 14, the bottom and top of the box indicate the first and third quartiles of the data, which contain the middle 50 percent of the data, and the length of the box reflects the degree of concentration of the data; the upper and lower whiskers mark the range of extreme values. Changes in the median (the middle line of the box) show the main trend, and the offset of the dotted line reveals the characteristics of the data distribution.

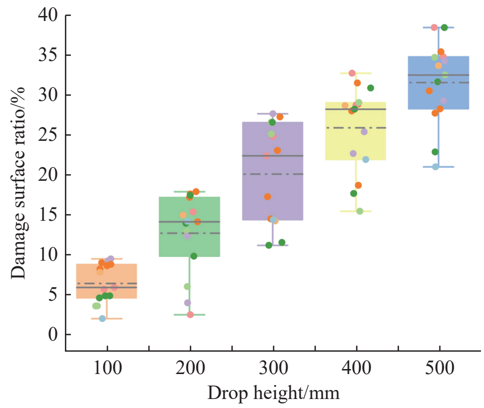

Figure 14 Test damage surface ratio

Analysis of the box-plot data shows that a one-way ANOVA confirms a significant overall effect of height on the damage surface ratio, $F(4, 70)=61.46$, $p<0.0001$, $\eta^2=0.78$. Tukey's HSD test, as summarized in Table 4, shows that all p-values are below the 0.05 significance level, indicating significant differences in damage between the heights and a monotonic increase in damage from 100 mm to 500 mm. The increase from 200 mm to 300 mm is particularly pronounced, whereas the increases from 300 mm to 400 mm and from 400 mm to 500 mm are statistically significant but more gradual.

Table 4 Tukey's HSD pairwise comparisons of damage surface ratio

Comparison/mm	Mean difference/%	Adjusted p-value
100 vs 200	+6.29	0.008
200 vs 300	+7.47	0.001
300 vs 400	+5.79	0.018
400 vs 500	+5.68	0.021

The stage-wise changes can be described in more detail as follows:

Low-height stage (100-200 mm): at 100 mm, the data were concentrated and the interquartile spacing was small, and the damage was stable; at 200 mm, there were anomalously low values and the data dispersion increased sharply, indicating that there was uncertainty in the damage response.

Mid-height stage (300 mm): the median is significantly higher and the data distribution is scattered, indicating that the damage is intensified and the volatility of the results is enhanced.

High-height stage (400-500 mm): the median peaked with a wide range of bins, indicating that the extreme difference of the data widened, showing that the damage surface ratio increased as a whole, but the individual differences were significant.

The results in Figure 14 show a nonlinear impact response of blueberry fruit. At a drop height of around 300 mm, both the damage surface ratio and its variability rise sharply, indicating that the impact energy reaches a critical threshold that induces bruising. Above 300 mm, the damage surface ratio continues to increase, but the growth rate gradually decreases. This behavior further supports the nonlinear collision dynamics model. Before the threshold is reached, the fruit exhibits strong resistance; once exceeded, the damage escalates rapidly and then increases more gradually.

Due to the difficulty of obtaining true 3D damage volume, this study uses the 2D damage surface ratio from cross-sections as an approximate indicator. This simplification may underestimate internal bruising and introduce random error when the cutting plane does not align with the damage center. Nevertheless, it effectively captures the trend of increasing damage with impact energy and supports the identification of 300 mm as a clear damage threshold. Future work may use X-ray CT, MRI, or 3D reconstruction to improve internal damage quantification.

The experimentally measured data were compared with the data measured by finite element simulation analysis and the results are shown in Figure 15. The analysis revealed that the maximum error was around 9%, which may be due to random fluctuations in size and ripeness among individual fruits. This experimental result fully proves the reasonableness of the finite element simulation analysis results.

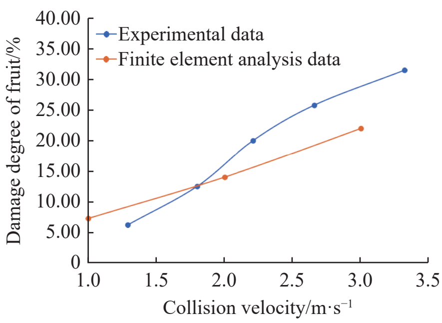

Figure 15 Comparison between simulation and experimental results

5 Conclusions

In this study, the mechanical behavior of blueberry fruit and its damage mechanism during the collision were studied from the perspectives of the mechanical model, simulation analysis, and collision experiment. Through the combination of theoretical analysis, simulation, and experimental verification, the mechanical behavior and damage mechanism of fruit collision are revealed, and the main conclusions of the study are as follows:

1) A nonlinear collision dynamics model of the fruit was established to obtain the collision forces during the mechanical harvesting of blueberries related to deformation, recovery coefficient, and collision velocity.

2) A discrete element simulation model of blueberry fruit is constructed to obtain two types of collision, fruit-rigid plate and fruit-fruit, in the process of fruit shedding. These two types of finite element models are constructed separately for comparison, and the analyses obtain that in the fruit-rigid plate collision model, the flesh of the fruit is subjected to greater stresses due to the high hardness of the rigid plate, which is more prone to plastic deformation than the fruit-fruit collision. It was obtained that the peak contact stress increased from 64 000 Pa to 110 000 Pa, the peak collision force increased from 1.85 N to 6.75 N, and the damage volume increased from 152.72 mm^3 to 459.42 mm^3 in the fruit-rigid plate collision model when the collision speed increased from 1 m/s to 3 m/s. It was found that the high-speed collision would lead to a significant expansion of the damage area inside the fruit.

3) Through the collision test, the maximum collision force that the blueberry fruit can withstand was obtained to be about 2-3 N. With the increase of the falling height, the collision force on the blueberry fruit increased rapidly, and when falling at a height of more than 300 mm, the collision force will be more than the structural endurance of the fruit. Furthermore, the surface ratio of the damage is positively correlated with the falling height, so the collision speed is a key factor that affects the collision behavior of fruit and the degree of damage. The reasonableness of the conclusion is verified by comparing the experimental data with the finite element simulation results.

The research in this paper provides an important theoretical basis and practical guidance for optimizing the design of fruit harvesting machinery and reducing fruit damage. Future research could further explore a wider range of mechanical fruit harvesting options by combining more fruit species and harvesting conditions.

Acknowledgements

This work was financially supported by the Collaborative Innovation Project of Disciplines in Heilongjiang Province (Grant No. LJGXCG2022-075) and the Postdoctoral Scientific Research Development Fund of Heilongjiang Province (Grant No. LBH-Q21020).

[References]

[1] Jiménez-Jiménez F, Castro-García S, Blanco-Roldán G L, Ferguson L, Rosa U A, Gil-Ribes J A. Table olive cultivar susceptibility to impact bruising. Postharvest Biology and Technology, 2013; 86: 100–106.

[2] Stopa R, Szyjewicz D, Komarnicki P, Kuta Ł. Determining the resistance to mechanical damage of apples under impact loads. Postharvest Biology and Technology, 2018; 146: 79–89.

[3] Yan D, Luo L F, Zhang P, Liu W T, Wang J X, Lu Q H, et al. Vibration analysis and experimental study of the effects of mechanised grape picking on the fruit–stem system. Biosystems Engineering, 2023; 227: 82–94.

[4] Hussein Z, Fawole O A, Opara U L. Preharvest factors influencing bruise damage of fresh fruits – A review. Scientia Horticulturae, 2018; 229: 45–58.

[5] Hu S W, Guo X L. A dissipative contact force model for impact analysis in multibody dynamics. Multibody Syst Dyn, 2015; 35: 131–151.

[6] Alaci S, Filote C, Ciornei F-C, Grosu O V, Raboaca M S. An analytical solution for non-linear viscoelastic impact. Mathematics, 2021; 9(6): 1849.

[7] Zheng Q J, Zhu H P, Yu A B. Finite element analysis of the contact forces between a viscoelastic sphere and rigid plane. Powder Technology, 2012; 226: 130–142.

[8] Lapshin V L, Zenkov E V, Yashenko V P. A three-mass viscoelastic plastic model used for studying mechanics and dynamics of shock interaction of solid bodies in determining the mechanical characteristics of building materials. IOP Conf Ser: Earth Environ Sci, 2021; 751: 012103.

[9] Yousefi S, Farsi H, Kheiralipour K. Drop test of pear fruit: Experimental measurement and finite element modelling. Biosystems Engineering, 2016; 147: 17–25.

[10] Dintwa E, Van Zeebroeck M, Ramon H, Tijskens E. Finite element analysis of the dynamic collision of apple fruit. Postharvest Biology and Technology, 2008; 49(2): 260–276.

[11] Wang W Z, Zhang S M, Fu H, Lu H Z, Yang Z. Evaluation of litchi impact damage degree and damage susceptibility. Computers and Electronics in Agriculture, 2020; 173: 105409.

[12] Zhang S M, Wang W Z, Wang Y F, Fu H, Yang Z. Improved prediction of litchi impact characteristics with an energy dissipation model. Postharvest Biology and Technology, 2021; 176: 111508.

[13] Du D D, Wang B, Wang J, Yao F Q, Hong X Z. Prediction of bruise susceptibility of harvested kiwifruit (*Actinidia chinensis*) using finite element method. Postharvest Biology and Technology, 2019; 152: 36–44.

[14] Hou J, Park B, Li C, Wang X. A multiscale computation study on bruise susceptibility of blueberries from mechanical impact. Postharvest Biology and Technology, 2024; 208: 112660.

[15] Cao J L, Bai X P, Xu D C, Li W B, Chen C C. Experiment and analysis on walnut (*Juglans regia* L.) shedding force based on low-frequency vibration response. Industrial Crops and Products, 2023; 204: 117242.

[16] Zhuo P, Li Y X, Wang B S, Jiao H B, Wang P, Li C S, et al. Analysis and experimental study on vibration response characteristics of mechanical harvesting of jujube. Computers and Electronics in Agriculture, 2022; 203: 107446.

[17] Lyu X M, Wang H B, Xu G F, Chu C. Research on fruit picking test of blueberry harvesting machinery under transmission clearance. Heliyon, 2024; 10(15): e34740.

[18] Diels E, Odenthal T, Keresztes J, Vanmaercke S, Verboven P, Nicolaï B, et al. Development of a visco-elastoplastic contact force model and its parameter determination for apples. Postharvest Biology and Technology, 2016; 120: 157–166.

[19] Lu R, Puri V M. Characterization of nonlinear creep behavior of two food products. Journal of Rheology, 1991; 35: 1209–1233.

[20] Bao Y D, Yang J, Zhao Y L, Liu X L, Liang Z, Guo Y L. Numerical simulation of mechanically harvested blueberry based on EDEM. Journal of Harbin University of Science and Technology, 2020; 25(3): 88–93. (in Chinese).